ACS APPLIED MATERIALS & INTERFACES

Research Article

www.acsami.org

Layered Double Hydroxide Assemblies with Controllable Drug Loading Capacity and Release Behavior as well as Stabilized Layer-by-Layer Polymer Multilayers

Fengzhu Lv,* Linan Xu, Yihe Zhang,* and Zilin Meng

Beijing Key Laboratory of Materials Utilization of Nonmetallic Minerals and Solid Wastes, National Laboratory of Mineral Materials, School of Materials Science and Technology, China University of Geosciences, Beijing, 100083, China

Supporting Information

ABSTRACT: A stable drug release system with magnetic targeting is essential in a drug delivery system. In the present work, layered double hydroxide assemblies stabilized by layer-by-layer polymer multilayers were prepared by alternative deposition of poly(allylamine hydrochloride) and poly(acrylic acid) species on composite particles of Fe_3O_4 and ZnAl-LDH and then covalent cross-linkage of the polymer multilayers by photosensitive cross-linker. The successful fabrication was recorded by Zeta potential and Fourier transform infrared spectrum measurements. The formed assemblies were stable in high pH solutions (pH > 7). The drug loading capacity and release behavior of the assemblies could be controlled by treatment with appropriate acidic solution, and were confirmed by loading and release of a simulated drug, methylene blue. The formed assemblies possessed enough saturated magnetic strength and were sensitive to external magnetic field which was essential for targeting drug delivery. The formed assemblies were multifunctional assemblies with great potential as drug delivery system.

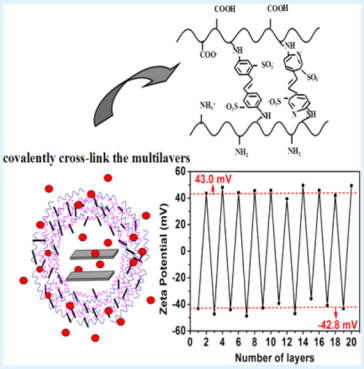

KEYWORDS: *Layered double hydroxide, layer-by-layer, covalent stabilization, etching, controlled drug release*

INTRODUCTION

Layered double hydroxide (LDH) is a hydrotalcite-like material with exchangeable anions in the interlayer of the positive brucite-like sheets. It has been extensively researched in biomedicine-related fields, such as drug delivery and release, due to its biocompatibility[1−4] and colloidal stability.[5−7] Additionally, LDH is easily degraded in acidic environments.[8] Smart LDH nanohybrids show even more superiority; among which magnetic LDH nanocomposites display promising properties as drug vehicles due to their targeted drug delivery by magnetic manipulation.[9]

Zhang's group[10,11] prepared core/shell magnetic LDHs through in situ coprecipitation, where the LDH shells wreathed the magnetic nanoparticle cores, and presented a pulsating drug release behavior toward an on/off alternative magnetic field. Recently, they improved the magnetic response of the magnetic LDHs by alternating the magnetic nanoparticle cores with magnetic clusters.[12] Although introduction of magnetic particles on LDH increases its response to external stimulation, it brings about another disadvantage. The introduction of magnetic particles on LDH decreases the stability of LDH colloids due to the magnetic attraction of inter particles, so the nanoparticles must be coated to prevent dissolution and aggregation of magnetic nanoparticles under physiological conditions (i.e., neutral pH and high salt concentration), to protect against protein adsorption. As such, improvement of the stability of magnetic LDHs in aqueous solution by surface modification with organic species is essential.

Layer-by-layer (LbL) technique is a widely explored facile nanofabrication method in construction of functional devices or systems.[13,14] The technique involves the alternative deposition of species with complementary groups for chemical interactions and could be employed effectively for interfacial modification of particles.[15,16] The Lin group[17] modified the surface of lignocellulosic fibers by LbL technique to increase their thermal stability. Moya's group[18] adsorpted positive or negative polyelectrolytes on nanotubes to prepare polyelectrolyte-coated carbon nanotubes. In the present work, composite particles of Fe_3O_4 and ZnAl(SDS)-LDH (Fe_3O_4/ZnAl-LDH) were used as drug delivery systems and their surface was modified by LbL deposition of poly(allylamine hydrochloride) (PAH) and poly(acrylic acid) (PAA). However, because the interlayer driving forces involved in LbL assemblies are generally weak supramolecular interactions, the stability of the assemblies also needs to be improved to widen their applications under extreme conditions. In general, converting the interlayer forces from weak supramolecular interactions to strong covalent bonds is an efficient way. Among the applied methods, post-cross-linkage of the as-prepared assembles is an easily performed method. Generally, linkable groups such as thermo-cross-linkable amino and carboxylic groups[19,20] and photo-cross-linkable phenyl azido[21] and diazonium groups[22]

Received: January 13, 2015
Accepted: August 3, 2015
Published: August 3, 2015

DOI: 10.1021/acsami.5b04569
ACS Appl. Mater. Interfaces 2015, 7, 19104−19111

are introduced in the block of LbL for post-cross-linkage. Among these, the formation of stable LbL films using phenyl azido groups is the most broadly used way because phenyl azido groups can easily photolyze upon UV irradiation to generate highly reactive nitrene intermediates that react with almost all kinds of organic matters to form covalent bonds.[23] Recently, small molecules with double post-linkable groups were used to stabilize LbL films. Glutaraldehyde[24,25] or epichlorohydrin[26] were used as cross-linking agents to accomplish the bridging of amino groups in the building blocks to obtain stabilized multilayers. Our group has used the small photosensitive molecule 4,4′-diazostilbene-2,2′-disulfonic acid disodium salt (DAS) as a post-linkage agent to modify magnetic MMT.[15]

In the present work, Fe_3O_4/ZnAl-LDH composite particles with pH responsibility and large drug capacity were modified by LbL of PAH and PAA and then stabilized by DAS though post-photolinkage. The drug loading ability and release behavior of the covalently LbL stabilized LDHs toward a simulated drug, methylene blue (MB), could be adjusted by treatment with acidic and basic solutions and was monitored by UV−vis measurement. The as-prepared assemblies possessed not only magnetic response ability, but also adjustable drug loading ability. Even more, the formed assemblies were stable under physiological conditions due to the LbL modification. The prepared LDH assemblies are a stable multifunctional drug release system with controllable drug loading capacity and release behavior.

EXPERIMENTAL SECTION

Materials. PAH (M_w = 15 000) was purchased from Sigma-Aldrich. PAA (M_w = 240 000, 25% aqueous solution) was obtained from Polysciences. DAS was purchased from TCI. MB was from Jingwen Chemical Reagent Co., Ltd. All other chemicals and reagents were obtained from Sinopharm Chemical Reagent Beijing Co., Ltd. (Beijing, China). The reagents were all analytical grade and used without further purification. Fe_3O_4/ZnAl-LDH composite particles with a M_s of 4.40 emu/g were synthesized in our lab.[27]

Characterization and Measurements. Zeta-potential values and particle size were measured using Zetasizer Nano ZS90 of Malvern Instruments Ltd. Field emission scanning electron microscopy (FE-SEM) images were acquired from a LEO-1530 operated at 5 kV. Transmission electron microscopy (TEM) imaging was carried out on an FEI TECNAI G220 transmission electron microscope. Atomic force microscopy (AFM) measurements were performed with a Nano Wizard atomic force microscope (SPA400 Probe Scan Microscope, Japan). The Fourier transform infrared (FTIR) spectra in the 4000−400 cm^{-1} region were obtained using a Perkin Elmer Spectrum 100 FT-IR spectrometer. KBr was used as a background material and disks of samples/KBr mixtures were prepared to obtain the FT-IR spectra. UV−vis spectra were obtained on a UV-765 spectrophotometer. The magnetization, M_s, was measured by a PTMS-9T Vibrating Sample Magnetometer at room temperature.

Preparation of Fe_3O_4/ZnAl-LDH. Seventy-five mL of a solution containing 0.02 mol $Zn(NO_3)_2{\cdot}6H_2O$, 0.01 mol $Al(NO_3)_3{\cdot}9H_2O$, and 75 mL of sodium dodecyl sulfonate (SDS, 3.0 g) solution were added to a solution containing a certain amount of Fe_3O_4 at a pH of 10. The mixture was aged at 65 °C for 8 h. The resulting precipitates were filtered, washed by deionized water, and dried at 70 °C.

Partial Exfoliation of Fe_3O_4/ZnAl-LDH. The synthesized Fe_3O_4/ZnAl-LDH (0.1 g) was dispersed in formamide (0.1 L). The mixture then was sonicated (Branson 5510 ultrasonic water bath, 180 W, 40 kHz) three times in successive intervals of 5 min. Following this treatment, the suspension was vigorously stirred for 72 h at 25 °C. Finally, the resulting translucent colloidal suspension was characterized and used for fabrication of the assemblies.[13]

Preparation of Covalently LbL Modified Magnetic (PAA/PAH)$_{10}$-LDH. The Fe_3O_4/ZnAl-LDH particles obtained by magnetic separation from 1 mg/mL suspension were added into PAA (1 mg/mL, pH = 6) solution for 10 min with agitation. After collection by centrifuge, the particles were washed by using dispersion-centrifuge in deionized water for 3 cycles. The particles were then immersed in a solution of PAH (4 mg/mL, pH = 9) also for 10 min and washed as the process for PAA. The above two processes were performed successively until intended multilayers were obtained. After the surface modification, thorough DAS was infiltrated into the multilayers by dispersion of the samples in an aqueous solution of DAS (5 mg/mL, pH = 3.8) for 1 h. The samples were then dried and subjected to UV irradiation by a UV lamp of 500 W from a distance of 20 cm for 1 h to covalently cross-link the multilayers. The obtained magnetic DAS-(PAA/PAH)$_{10}$-LDH assemblies were immersed in basic (pH = 10−11) and acidic (pH = 2−3) solutions separately for 5 and 1 h to form LDH assemblies with different drug loading ability, and the corresponding assemblies were assigned as B-DAS-(PAA/PAH)$_{10}$-LDH and A-DAS-(PAA/PAH)$_{10}$-LDH, respectively. The control sample, which was not further stabilized by DAS, was assigned as (PAA/PAH)$_{10}$-LDH.

Loading and Release of MB. Loading of MB was realized by immersion of magnetic LDH assemblies into aqueous solution of MB (8×10^{-3} mg/mL) for 24 h. The samples loaded with MB were then immersed into PBS (pH = 7.4, 10 mM, 16 mL). After a 24-h interval, a magnet was put close to the bottom of the vial to give supernatant in the upper layer of the vial. Then 4 mL of the supernatant solution was taken for UV−vis measurement and returned to the vial afterward. The measurements were carried out until the absorbance of the supernatant solution was stable for at least 3 days. Every supernatant solution was measured three times and the averages of the values were used to obtain the release profiles.

RESULTS AND DISCUSSION

Partial Exfoliation of Fe_3O_4/ZnAl-LDH. The synthesized Fe_3O_4/ZnAl-LDH was first exfoliated in formamide to form colloids with different concentrations. The stability of the colloids with time was determined by turbidity measurement and is shown in Supporting Information (SI) Figure s1. The turbidity of the colloids with concentration of 0.05−0.5 wt % Fe_3O_4/ZnAl-LDH all decreased, showing a relatively higher turbidity change compared to some reports about clays.[28,29] As the concentration of Fe_3O_4/ZnAl-LDH was 0.05 wt %, the turbidity changed about 150 within 30 min, indicating a comparatively stable colloid formed. The particle size of 0.05 wt % of Fe_3O_4/ZnAl-LDH colloids was determined to be about 700 nm (medium particle size) according to their particle size dispersion shown in Figure1a; the width of ZnAL(SDS)-LDH sheets observed by SEM was about 300 nm (Figure s2).[27] So, in the colloids, Fe_3O_4/ZnAl-LDH existed as partial exfoliated assemblies with the interlayer space preserved. This conclusion also was confirmed by AFM measurement. The AFM tapping mode images in Figure 2a and 2c showed the height of LDH was about 13 nm before exfoliation. After exfoliation, the height of the nanosheets (Figure 2b and 2d) varied from a minimum of 1.53 to about 2.71 nm. Considering the known thickness of the brucite-type layers of LDHs with organic intercalators was between 0.7 and 2.5 nm,[30] Fe_3O_4/ZnAl-LDH was partially exfoliated to two or three layers with some of the interlayer space preserved, which was the place of drug loading. Then the partially exfoliated Fe_3O_4/ZnAl-LDH was surface-modified by LbL to further improve the stability of the assemblies.

Fabrication of Stable LDH Assemblies by LbL Process. To prepare assemblies with partially exfoliated Fe_3O_4/ZnAl-LDH as cores and polymer multilayers around the LDHs as shell by LbL technique, the Fe_3O_4/ZnAl-LDH were dispersed

DOI: 10.1021/acsami.5b04569
ACS Appl. Mater. Interfaces 2015, 7, 19104−19111

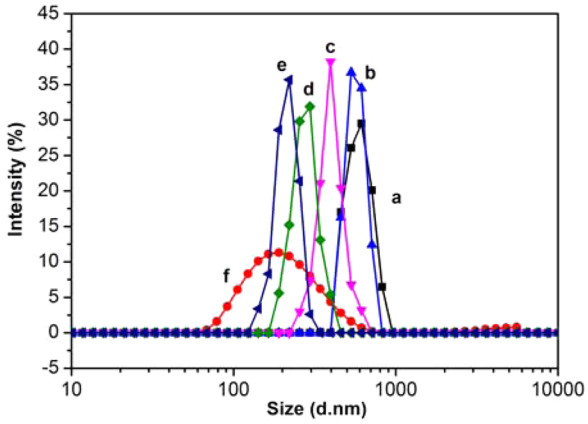

Figure 1. Particle size of (a) Fe_3O_4/ZnAl-LDH, (b) DAS-$(PAA/PAH)_{10}$-LDH, and DAS-$(PAA/PAH)_{10}$-LDH colloids after treatment by a solution with pH of 2−3 for (c) 0.5 h, (d) 1 h, (e) 1.5 h, and (f) by a solution with pH below 1 for 12 h.

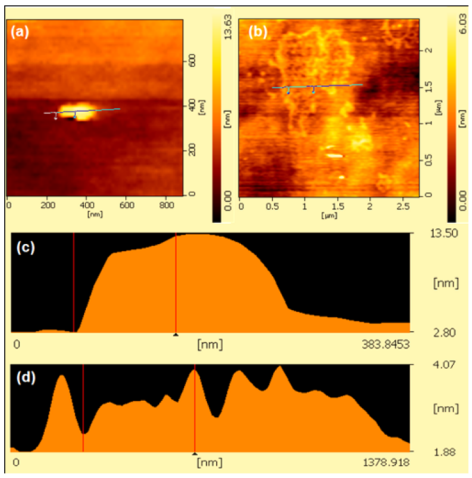

Figure 2. AFM images of Fe_3O_4/ZnAl-LDH (a) before and (b) after being exfoliated in formamide and (c, d) height profile along the lines in images (a) and (b).

alternatively in aqueous solutions of PAA (1 mg/mL, pH = 6) and PAH (1 mg/mL, pH = 9) until the core−shell structure of $(PAA/PAH)_{10}$-LDH was obtained. The immersion time for each step was 10 min. Between successive steps, the composite particles were thoroughly washed with deionized water using three dispersion-centrifuge cycles. The fabrication process is illustrated in Figure 3. The surface-potential (zeta-potential) of the composite particles shown in Figure 4 switched alternately between −42.8 mV and +43 mV, demonstrating the alternative switching of the LDH surface with PAA and PAH, as well as the successful formation of core−shell assemblies. Meanwhile ,the high absolute zeta-potentials showed that the formed assemblies were still stable colloids in water.

The successful modification of LDHs by 10 layers of PAA/PAH was also confirmed by FT-IR spectra as shown in Figure 5. In Figure 5a, the broad adsorption band at 3500 cm^{-1} is vibration of structural water within the LDH interlayer. The characteristic symmetric and asymmetric stretching vibrations of $-CH_2$ at 2918 and 2851 cm^{-1}, and the vibrations around 1207 and 1120 cm^{-1}, were ascribed to SDS molecules intercalated in the LDH interlayers. The peak around 580 cm^{-1} was assigned to the stretching vibrational peak of Fe−O bond in Fe_3O_4 nanoparticles. After LbL modification of the LDHs (Figure 5b), the characteristic peak of COO^- appeared around 1558 cm^{-1}, and the less intense peak on its shoulder at around 1620 cm^{-1} was attributed to $-NH_2$.[31] The appearance of the vibrational bands corresponding to COO^- and NH_2 indicated that PAA/PAH multilayers were successfully fabricated around the LDH cores. However, as the multilayers around LDH cores could disassemble if the assemblies were immersed in water or acidic or basic solution for a long time, the outer layer of the assemblies was further cross-linked by DAS to widen their applications in certain circumstances. After immersion in DAS (5 mg/mL) for 1 h, the characteristic vibrational band corresponding to azide groups around 2100 cm^{-1} in the FT-IR of Figure 5c appeared demonstrating that DAS permeated into LDH assemblies.[32] Then the outer layer of the assemblies was cross-linked by UV-induced photochemical cross-linking.[33] After UV irradiation for 1 h, the characteristic peaks of the cross-linked (PAA/PAH)10-LDH had no obvious change with its precursor (Figure 5d) except the lowered vibrational peak of azide groups. Under UV irradiation, a large amount of DAS decomposed to generate nitrenes, resulting in the decrease of the vibrational intensity of azide groups. Then, the nitrene species would react with their adjacent groups in an unselective manner, to generate covalent bonds.[34,35] Thus, just as shown in Figure 3, the polymer multilayers were stabilized by covalent cross-linkage.

The particle size and the size dispersion of the assemblies after stabilization by covalent LbL layers (shown in Figure 1b) almost did not change compared to its LDH precursors (Figure 1a). These data indicate the covalent LbL modification mainly took place on the surface of individual assemblies and the size of the target particles was not influenced by the LbL process. So the further combination of assemblies was not dominant in the LbL process.

The morphology and composition of the DAS-$(PAA/PAH)_{10}$-LDH assemblies are shown in Figure 6. The SEM showed DAS-$(PAA/PAH)_{10}$-LDH existed as polydispersed assemblies (Figure 6a). The connection between assemblies is not obvious. For one assembly it is irregular particles with more wrinkles due to the partial exfoliation (Figure 6b). The composition of the assemblies was further analysized by EDS analysis (Figure 6c). The EDS data (Table s1), which reflected the surface composition of the particles, showed that high content of C, S, and especially N elements appeared. As only PAH contained N elements in the building blocks, so polymer multilayers loaded on LDHs and the target particles possessed core−shell structure.

The XRD patterns of the prepared DAS-$(PAA/PAH)_{10}$-LDHs (Figure 7b) displayed the characteristic peaks of lamellar structure of LDHs corresponding to (003), (006), and (009) crystalline faces.[36] Meanwhile the (003) crystalline peak corresponding to the basal spacing of LDHs was still at lower angle ($2\theta = 3.4°$) than its precursors (Figure 7a), showing that SDS was still in the interlayers of LDHs, and LDHs still had the ability of loading drugs in the interlayers. The LbL and cross-linking process had little effect on the core structure.

Sensibility of the LDH Assemblies to Acid and Base. As the protective polymer multilayers are cross-linked by covalent bonds, generally it is stable in acidic and basic solutions; but, as LDH is acid sensitive,in acidic solution the LDH cores of the stabilized LDH assemblies could be etched gradually, finally resulting in the collapse of the LDH assemblies. As the LDH assemblies were immersed in acidic

DOI: 10.1021/acsami.5b04569
ACS Appl. Mater. Interfaces 2015, 7, 19104−19111

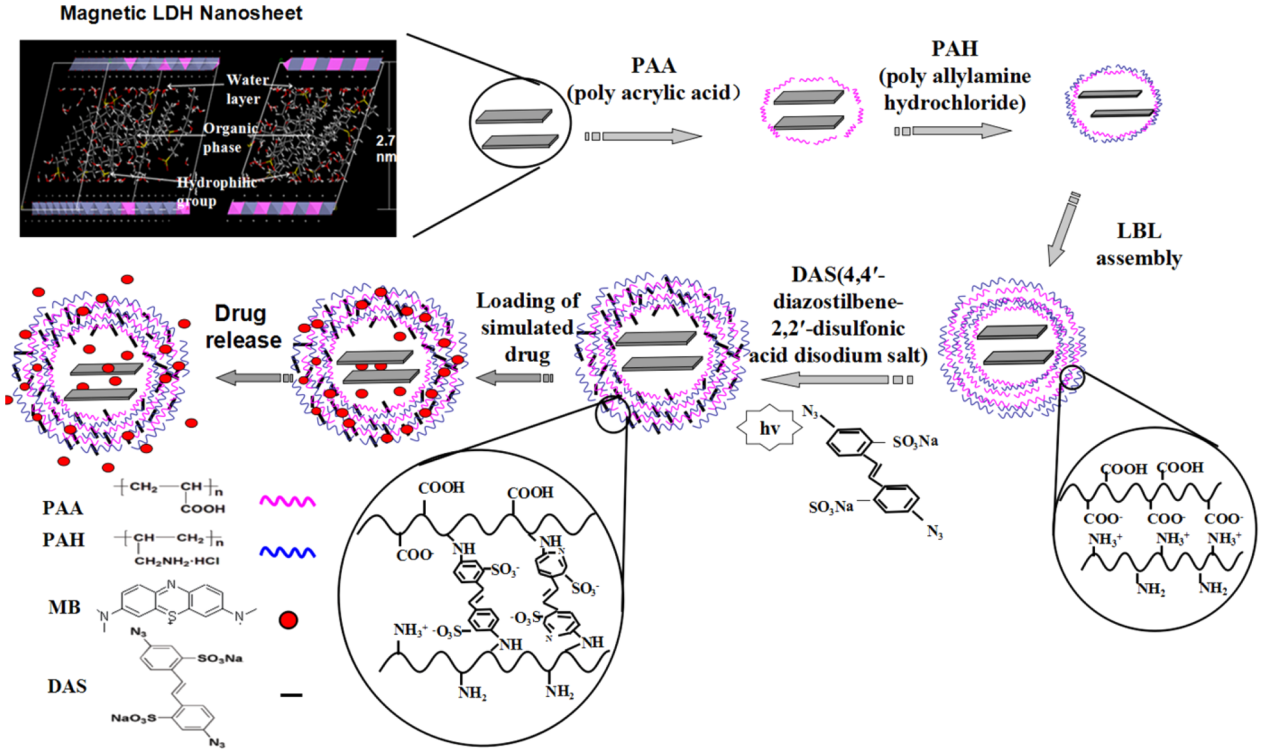

Figure 3. Illustration for the fabrication of stabilized ZnAl-LDH via LbL process.

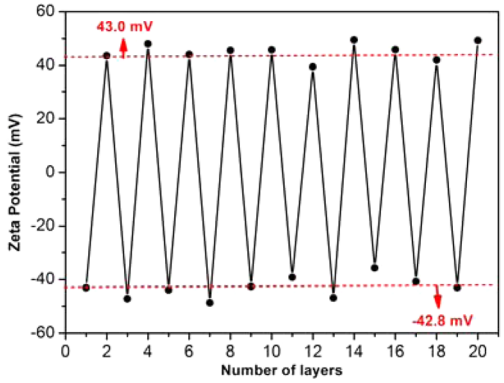

Figure 4. Zeta-potential as a function of successive LbL.

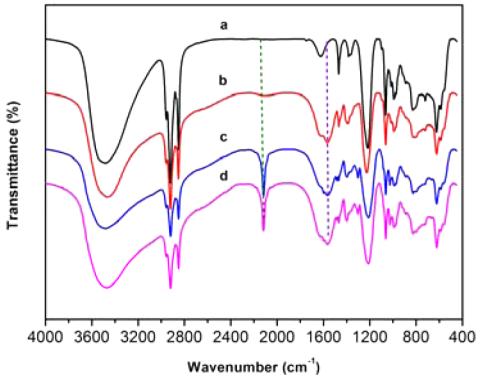

Figure 5. FT-IR absorption spectra of (a) Fe_3O_4/ZnAl-LDH, (b) $(PAA/PAH)_{10}$-LDH, and DAS-$(PAA/PAH)_{10}$-LDH (c) before and (d) after UV irradiation.

solution with pH = 2−3 ($[H^+]$ = 0.01−0.001 mol/L) for less than 60 min, the continued existence of the obvious vibrational

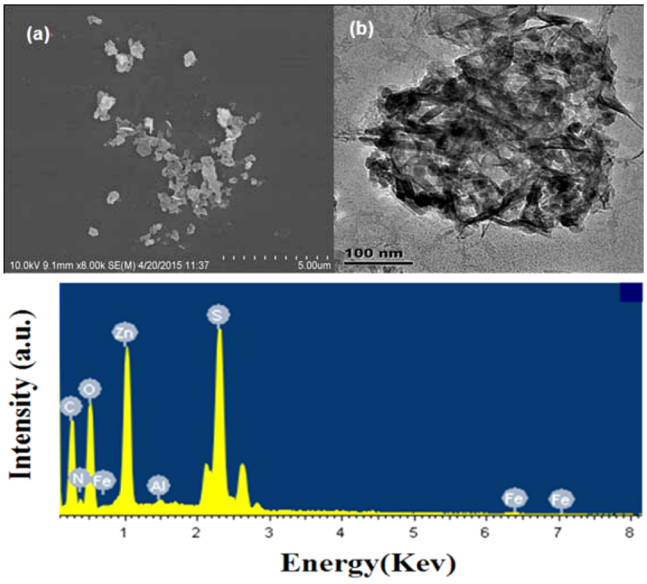

Figure 6. (a) SEM, (b) TEM images, and (c) EDS analysis of DAS-$(PAA/PAH)_{10}$-LDH.

bands corresponding to COO^- and NH_2 (shown in Figure 8) indicated that the LDH assemblies were still stable. But as the immersion time was as long as 60 min, the vibrational band corresponding to COOH at 1720 cm^{-1} appeared[25] and the vibrational band of NH_2 (1620 cm^{-1}) was more obvious. These data indicated that as the LDH assemblies were immersed in acid for enough time the polymer shell would expand and the electrostatic adsorption between the carboxyl and NH_3^+ groups was weakened, resulting in the partial etching of LDH cores.[9] The particle size (medium particle size) of DAS-$(PAA/PAH)_{10}$-LDH decreased to 396, 287, and 220 nm from 700 nm as the

DOI: 10.1021/acsami.5b04569
ACS Appl. Mater. Interfaces 2015, 7, 19104−19111

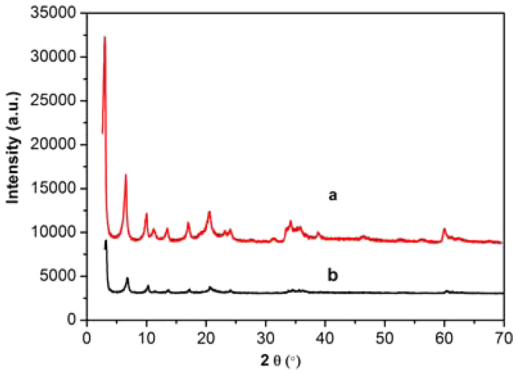

Figure 7. XRD patterns of (a) Fe_3O_4/ZnAl-LDH and (b) DAS-$(PAA/PAH)_{10}$-LDH.

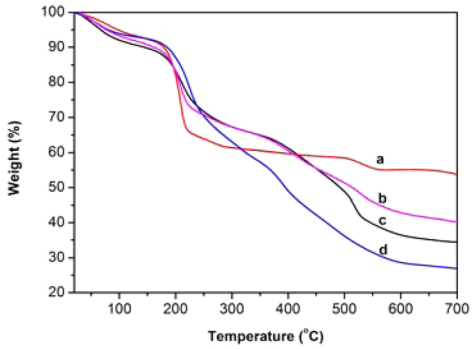

Figure 9. Weight loss of (a) Fe_3O_4/ZnAl-LDH, (b) B-DAS-$(PAA/PAH)_{10}$-LDH, (c) DAS-$(PAA/PAH)_{10}$-LDH, and (d) A-DAS-$(PAA/PAH)_{10}$-LDH.

etching time increased to 0.5, 1, and 1.5 h in pH = 2−3 solution. The particle size of the DAS-$(PAA/PAH)_{10}$-LDH after immersing in acid solution with pH below 1 for 12 h (Figure 1c) was greatly decreased, confirming the above speculation. So LDH assemblies treated by acid had smaller cores and changed drug loading ability compared to DAS-$(PAA/PAH)_{10}$-LDH assemblies. But as the stabilized LDH assemblies were treated with base (pH = 11−12) or aqueous solution for as long as 24 h, their FT-IR spectra had no obvious change, indicating that the assemblies were stable in these solutions. Figure 8b is the FI-IR spectra of base-treated DAS-$(PAA/PAH)_{10}$-LDH.

To understand if the polymer shell could be dissolved into the acidic or basic solutions, the weight loss of the assemblies before (Figure 9c) and after immersing in base (Figure 9b) and acid (Figure 9d) for 5 and 1 h, respectively, was measured. The weight loss of DAS-$(PAA/PAH)_{10}$-LDH (Figure 9c) showed loss behavior in three stages which ranged room temperature to 150, 180−250, and 250−550 °C. Just as Fe_3O_4/ZnAl-LDH (Figure 9a), the weight loss in the two lower temperature ranges corresponded to the removal of adsorbed water and the decomposition of the SDS in the interlayer of LDHs.[27] The weight loss in the higher temperature range between 250 and 550 °C was contributed by the degradation of the cross-linked polymer layers[37] and the collapse of the LDH layers. The weight loss of the base-treated assemblies (B-DAS-$(PAA/PAH)_{10}$-LDH) below 450 °C where organic composition completely decomposed almost overlapped that of DAS-$(PAA/PAH)_{10}$-LDH, indicating B-DAS-$(PAA/PAH)_{10}$-LDH and DAS-$(PAA/PAH)_{10}$-LDH had the same amount of organic compositions and base treatment had less effect on the polymer multilayers (Figure 9b). The weight loss of B-DAS-$(PAA/PAH)_{10}$-LDH after 520 °C was not as dominant as DAS-$(PAA/PAH)_{10}$-LDH, giving higher residue content. This may derive from the dense packing of B-DAS-$(PAA/PAH)_{10}$-LDH which results in incomplete degradation of the polymer shell and more C deposition on LDH. The weight loss of the assemblies treated by acid decreased almost linearly with temperature as the temperature was higher than 280 °C (Figure 9d). The weight loss of A-DAS-$(PAA/PAH)_{10}$-LDH cores was covered by the degradation of polymer layers. The residue weight of ZnAl(SDS)-LDH and the assemblies was in the order of ZnAl(SDS)-LDH > B-DAS-$(PAA/PAH)_{10}$-LDH > DAS-$(PAA/PAH)_{10}$-LDH > A-DAS-$(PAA/PAH)_{10}$-LDH, indicating that the organic content of the assemblies was in the inverse order as residue weight. These data further confirmed that as the assemblies were treated by acid, only the LDH cores were etched and the polymer shells were not obviously influenced.

Furthermore, the magnetic properties of the LDH assemblies were studied after organic modification by covalent LbL multilayers. The saturated value of the magnetic moment of DAS-$(PAA/PAH)_{10}$-LDH and B-DAS-$(PAA/PAH)_{10}$-LDH at 300 K was about 4.40 emu/g as shown in Figure 10a and 10b. But the saturation magnetization of A-DAS-$(PAA/PAH)_{10}$-LDH decreased to 1.28 emu/g, as the stability of Fe_3O_4 in acidic solution is weak.[9] It has been confirmed by our group that a montmorillonite (MMT) particle with 3.5 emu/g saturation magnetization could provide enough force under

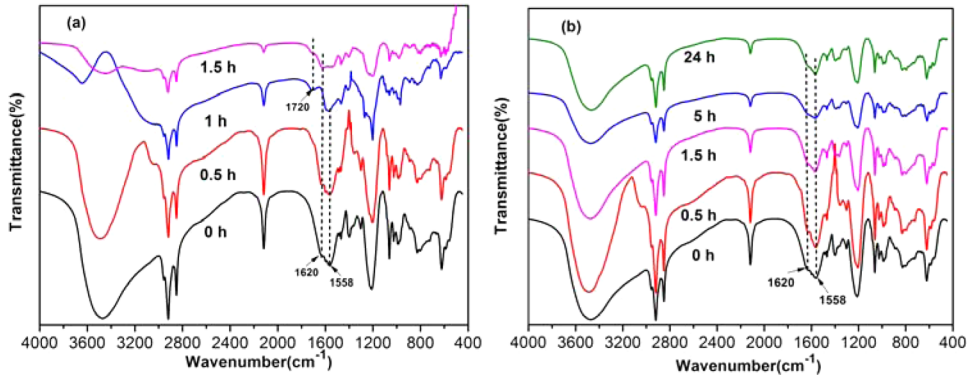

Figure 8. FT-IR absorption spectra of DAS-$(PAA/PAH)_{10}$-LDH after treatment by solutions with a pH value of (a) 2−3 and (b) 11−12 for different times.

DOI: 10.1021/acsami.5b04569
ACS Appl. Mater. Interfaces 2015, 7, 19104−19111

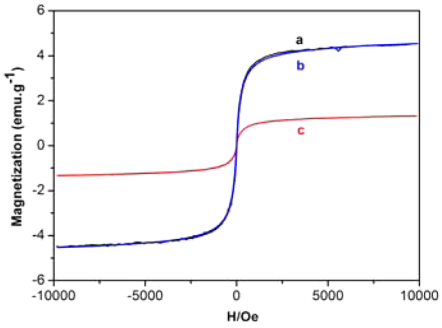

Figure 10. Magnetic hysteresis loops of (a) DAS-$(PAA/PAH)_{10}$-LDH, (b) B-DAS-$(PAA/PAH)_{10}$-LDH, and (c) A-DAS-$(PAA/PAH)_{10}$-LDH at room temperature.

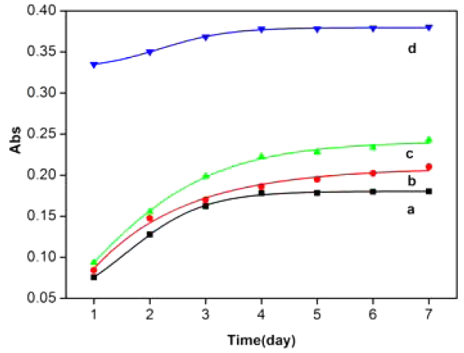

Figure 11. Release behavior of (a) $(PAA/PAH)_{10}$-LDH, (b) DAS-$(PAA/PAH)_{10}$-LDH, (c) B-DAS-$(PAA/PAH)_{10}$-LDH, and (d) A-DAS-$(PAA/PAH)_{10}$-LDH toward MB.

magnetic field to drag not only itself, but also 10^5 times its own weight of cargo, in a liquid environment.[15] The saturation magnetization of LDH assemblies was between 1.28 and 4.40 emu/g and in the same order of magnitude as MMT, so the prepared assemblies possessed enough saturation magnetization responsive to external magnetic force.[38,15] The as-prepared assemblies were a stable and magnet-responsive drug-release system.

Loading and Release of Simulated Drug. The loading amounts of MB on DAS-$(PAA/PAH)_{10}$-LDH and B-DAS-(PAA/PAH)10-LDH were 1.69 and 1.49 mg/g, respectively, lower than that of $(PAA/PAH)_{10}$-LDH whose loading amount was 1.90 mg/g. The decreased drug loading amount indicated DAS-$(PAA/PAH)_{10}$-LDH and B-DAS-$(PAA/PAH)_{10}$-LDH became more dense after cross-linking the outer layers and treatment by base which limited the further expansion of LDH cores as MB immersing in. Therefore, A-DAS-$(PAA/PAH)_{10}$-LDH was speculated as possessing a large cavity in LDH cores and could load more drugs due to the etching effect of acid on LDH cores. But the loading amount of DAS-$(PAA/PAH)_{10}$-LDH after etching in pH = 2−3 solution for 0.5 and 1 h decreased to 1.37 and 1.13 mg/g, respectively. Although part of LDH could be etched out, the particle size would decrease accordingly with etching time (Figure 1c, 1d, and 1e), but the polymer layers still adhered on the LDH cores due to their flexibility. Therefore, no large cavities were further introduced in A-DAS-$(PAA/PAH)_{10}$-LDH assemblies. In contrast, acidic treatment decreased the content of LDH cores and decreased the adsorption of A-DAS-$(PAA/PAH)_{10}$-LDH toward MB. So, in the target samples, DAS-$(PAA/PAH)_{10}$-LDH possessed the largest drug loading ability, but its drug loading ability decreased after base and acid treatment. The decrease degree became more obvious with the acid treatment time.

The drug release behavior from $(PAA/PAH)_{10}$-LDH, DAS-$(PAA/PAH)_{10}$-LDH, B-DAS-$(PAA/PAH)_{10}$-LDH, and A-DAS-$(PAA/PAH)_{10}$-LDH in PBS solution was studied and is shown in Figure 11. The in vitro release amount of MB from $(PAA/PAH)_{10}$-LDH (Figure 11a), DAS-$(PAA/PAH)_{10}$-LDH (Figure 11b), and B-DAS-$(PAA/PAH)_{10}$-LDH (Figure 11c) increased gradually and then almost leveled off. But the release of MB from A-DAS-$(PAA/PAH)_{10}$-LDH (Figure 11d) showed a very different behavior. The release rate was obviously higher than that of DAS-$(PAA/PAH)_{10}$-LDH and $(PAA/PAH)_{10}$-LDH. Most of the MB was released within 1 day. The release rate increase was due to the loose stacking of LDH layers which came from the etching in the acid treatment,[39] and was in accordance with the release behavior of general intercalated LDHs.[40,41] So $(PAA/PAH)_{10}$-LDH, DAS-$(PAA/PAH)_{10}$-LDH, and B-DAS-$(PAA/PAH)_{10}$-LDH were long-term drug release systems, while A-DAS-$(PAA/PAH)_{10}$-LDH was a fast release system. Thus, it is speculated that DAS-$(PAA/PAH)_{10}$-LDH treated by base and acid for different times possess different drug loading and release behaviors.

In summary, the drug loading capacity of DAS-$(PAA/PAH)_{10}$-LDH and its drug release behavior can be adjusted by acid and base treatments for different times. The prepared DAS-$(PAA/PAH)_{10}$-LDH assemblies are capable of use as drug delivery systems with controllable drug loading capacity and release behavior, with stabilized LbL shell layers as well as magnetic targeting function.

CONCLUSIONS

LDH assemblies with stabilized LbL shell layers were prepared by alternative deposition of PAH and PAA species on hybrid particles of Fe_3O_4 and layered double hydroxide and then covalent cross-linkage of the polymer shell by small photosensitive cross-linker molecules. The successful fabrication of the assemblies and the cross-linking of the polymer layers were recorded by Zeta potential and FT-IR measurement. The formed assemblies are stable in higher pH solutions (pH > 7). But the LDH cores can be partially etched to form assemblies with controlled drug loading capacity. Also, the release behavior of the assemblies can be adjusted by appropriate etching of the LDH cores by acid. These specific properties of the assemblies were confirmed by loading and release of the simulated drug MB. Also, the formed assemblies possessed enough saturated magnetic strength and were sensitive to external magnetic field which was essential to target drug delivery. The formed assemblies have great potential as drug release systems.

ASSOCIATED CONTENT

Supporting Information

The Supporting Information is available free of charge on the ACS Publications website at DOI: 10.1021/acsami.5b04569.

Figures showing SEM image and UV−vis spectrum of ZnAl(SDS)-LDH and the turbidity of ZnAl(SDS)-LDH solution, as well as the element composition of DAS-$(PAA/PAH)_{10}$-LDH (PDF)

AUTHOR INFORMATION

Corresponding Authors

* E-mail: lfz619@cugb.edu.cn.
*E-mail: zyh@cugb.edu.cn.

DOI: 10.1021/acsami.5b04569
ACS Appl. Mater. Interfaces 2015, 7, 19104−19111

Notes

The authors declare no competing financial interest.

■ ACKNOWLEDGMENTS

This work was supported by the Fundamental Research Funds for the Central Universities (2-9-2013-49 and 2-9-2014-123).

■ REFERENCES

(1) Gu, Z.; Atherton, J. J.; Xu, Z. P. Hierarchical Layered Double Hydroxide Nanocomposites: Structure, Synthesis and Applications. *Chem. Commun.* **2015**, *51*, 3024−3036.
(2) Gu, Z.; Zuo, H. L.; Li, L.; Wu; Xu, Z. P. Pre-Coating Layered Double Hydroxide Nanoparticles with Albumin to Improve Colloidal Stability and Cellular Uptake. *J. Mater. Chem. B* **2015**, *3*, 3331−3339.
(3) Yao, F.; Hu, H.; Xu, S. L.; Huo, R. J.; Zhao, Z. P.; Zhang, F. Z.; Xu, F. J. Preparation and Regulating Cell Adhesion of Anion-Exchangeable Layered Double Hydroxide Micropatterned Arrays. *ACS Appl. Mater. Interfaces* **2015**, *7*, 3882−3887.
(4) Wang, D. H.; Ge, N. J.; Li, J. H.; Qiao, Y. Q.; Zhu, H. Q.; Liu, X. Y. Selective Tumor Cell Inhibition Effect of Ni−Ti Layered Double Hydroxides Thin Films Driven by the Reversed pH Gradients of Tumor Cells. *ACS Appl. Mater. Interfaces* **2015**, *7*, 7843−7854.
(5) Rives, V.; del Arco, M.; Martin, C. Layered Double Hydroxides as Drug Carriers and for Controlled Release of Non-Steroidal Antiinflammatory Drugs (NSAIDs): A Review. *J. Controlled Release* **2013**, *169*, 28−39.
(6) Zhao, M. Q.; Zhang, Q.; Huang, J. Q.; Wei, F. Hierarchical Nanocomposites Derived from Nanocarbons and Layered Double Hydroxides-Properties, Synthesis, and Applications. *Adv. Funct. Mater.* **2012**, *22*, 675−694.
(7) Li, A.; Qin, L. L.; Zhu, D.; Zhu, R. R.; Sun, J.; Wang, S. L. Signalling Pathways Involved in the Activation of Dendritic Cells by Layered Double Hydroxide Nanoparticles. *Biomaterials* **2010**, *31*, 748−756.
(8) Li, C.; Wang, L. Y.; Wei, M.; Evans, D. G.; Duan, X. Large Oriented Mesoporous Self Supporting Ni-Al Oxide Films Derived from Layered Double Hydroxide Precursors. *J. Mater. Chem.* **2008**, *18*, 2666−2672.
(9) Li, D.; Zhang, Y. T.; Yu, M.; Guo, J.; Chaudhary, D.; Wang, C. C. Cancer Therapy and Fluorescence Imaging Using the Active Release of Doxorubicin from MSPs/Ni-LDH Folate Targeting Nanoparticles. *Biomaterials* **2013**, *34*, 7913−7922.
(10) Zhang, H.; Pan, D. K.; Zou, K.; He, J.; Duan, X. A Novel Core-Shell Structured Magnetic Organiceinorganic Nanohybrid Involving Drug-Intercalated Layered Double Hydroxides Coated on a Magnesium Ferrite Core for Magnetically Controlled Drug Release. *J. Mater. Chem.* **2009**, *19*, 3069−3077.
(11) Zhang, H.; Pan, D. K.; Duan, X. Synthesis, Characterization and Magnetically Controlled Release Behavior of Novel Core-Shell Structural Magnetic Ibuprofenintercalated LDH Nanohybrids. *J. Phys. Chem. C* **2009**, *113*, 12140−12148.
(12) Pan, D. K.; Zhang, H.; Fan, T.; Chen, J. G.; Duan, X. Nearly Monodispersed Coreeshell Structural Fe_3O_4@DFUR-LDH Submicro-particles for Magnetically Controlled Drug Delivery and Release. *Chem. Commun.* **2011**, *47*, 908−910.
(13) Dou, Y. B.; Han, J. B.; Wang, T. L.; Wei, M.; Evans, D. G.; Duan, X. Temperature-Controlled Electrochemical Switch Based on Layered Double Hydroxide/Poly(N-Isopropylacrylamide) Ultrathin Films Fabricated via Layer-by-Layer Assembly. *Langmuir* **2012**, *28*, 9535−9542.
(14) Zhou, Y.; Cheng, M. J.; Zhu, X. Q.; Zhang, Y. J.; An, Q.; Shi, F. A Facile Method to Prepare Molecularly Imprinted Layer-by-Layer Nanostructured Multilayers Using Postinfiltration and a Subsequent Photo-Cross-Linking Strategy. *ACS Appl. Mater. Interfaces* **2013**, *5*, 8308−8313.
(15) Xu, L. N.; Lv, F. Z.; Zhang, Y. H.; Luan, X. L.; Zhang, Q.; An, Q. Interfacial Modification of Magnetic Montmorillonite (MMT) Using Covalently Assembled LbL Multilayers. *J. Phys. Chem. C* **2014**, *118*, 20357−20362.
(16) Srivastava, S.; Kotov, N. A. Composite Layer-by-Layer Assembly with Inorganic Nanopartices and Nanowires. *Acc. Chem. Res.* **2008**, *41*, 1831−1841.
(17) Lin, Z.; Renneckar, S.; Hindman, D. P. Nanocomposite-Based Lignocellulosic Fibers 1. Thermal Stability of Modified Fibers with Clay-Polyelectrolyte Multilayers. *Cellulose* **2008**, *15*, 333−346.
(18) Moya, S. E.; Ilie, A.; Bendall, J. S.; Hernandez-Lopez, J. L.; Ruiz-García, J.; Huck, W. T. S. Assembly of Polyelectrolytes on CNTs by Van der Waals Interactions and Fabrication of LBL Polyelectrolyte/CNT Composites. *Macromol. Chem. Phys.* **2007**, *208*, 603−608.
(19) Olugebefola, S. C.; Kuhlman, W. A.; Rubner, M. F.; Mayes, A. M. Photopatterned Nanoporosity in Polyelectrolyte Multilayer Films. *Langmuir* **2008**, *24*, 5172−5178.
(20) Li, Q.; Quinn, J. F.; Caruso, F. Nanoporous Polymer Thin Films via Polyelectrolyte Templating. *Adv. Mater.* **2005**, *17*, 2058−2062.
(21) Wu, J. J.; Zhang, L.; Wang, Y. X.; Long, Y. H.; Gao, H.; Zhang, X. L.; Zhao, N.; Cai, Y. L.; Xu, J. Mussel-Inspired Chemistry for Robust and Surface-Modifiable Multilayer Films. *Langmuir* **2011**, *27*, 13684−13691.
(22) Sun, J. Q.; Wu, T.; Sun, Y. P.; Wang, Z. Q.; Zhang, X.; Shen, J. C.; Cao, W. X. Fabrication of a Covalently Attached Multilayer viaPhotolysis of Layer-by-Layer Self-Assembled Films Containing Diazo-Resins. *Chem. Commun.* **1998**, 1853−1854.
(23) Wu, G. L.; Shi, F.; Wang, Z. Q.; Liu, Z.; Zhang, X. Poly(acrylic acid)-Bearing Photoreactive Azido Groups for Stabilizing Multilayer Films. *Langmuir* **2009**, *25*, 2949−2955.
(24) Ren, K. F.; Ji, J.; Shen, J. C. Tunable DNA Release from Cross-Linked Ultrathin DNA/PLL Multilayered Films. *Bioconjugate Chem.* **2006**, *17*, 77−83.
(25) Tuong, S. D.; Lee, H.; Kim, H. Chemical Fixation of Polyelectrolyte Multilayers on Polymer Substrates. *Macromol. Res.* **2008**, *16*, 373−378.
(26) Dragan, E. S.; Bucatariu, F. Cross-Linked Multilayers of Poly(vinyl amine) as a Single Component and Their Interaction with Proteins. *Macromol. Rapid Commun.* **2010**, *31*, 317−322.
(27) Lv, F. Z.; Wu, Y. Y.; Zhang, Y. H.; Shang, J. W.; Chu, P. K. Structure and Magnetic Properties of Soft Organic ZnAl-LDH/Polyimide Electromagnetic Shielding Composites. *J. Mater. Sci.* **2012**, *47*, 2033−2039.
(28) Ersoy, B. Effect of pH and Polymer Charge Density on Settling Rate and Turbidity of Natural Stone Suspensions. *Int. J. Miner. Process.* **2005**, *75*, 207−216.
(29) Katz, A. L.; Xu, M.; Steiner, J. C.; Trusiak, A.; Alimova, A.; Gottlieb, P.; Block, K. Influence of Cations on Aggregation Rates in Mg-Montmorillonite. *Clays Clay Miner.* **2013**, *61*, 1−10.
(30) Guo, Y.; Zhang, H.; Zhao, L.; Li, G. D.; Chen, J. S.; Xu, L. Synthesis and Characterization of Cd−Cr and Zn−Cd−Cr Layered Double Hydroxides Intercalated with Dodecyl Sulfate. *J. Solid State Chem.* **2005**, *178*, 1830−1836.
(31) Tuong, S. D.; Lee, H.; Kim, H. Chemical Fixation of Polyelectrolyte Multilayers on Polymer Substrates. *Macromol. Res.* **2008**, *16*, 373−378.
(32) Lieber, E.; Ramachandra Rao, C. N. R.; Chao, T. S.; Hoffman, C. W. W. Infrared Spectra of Organic Azides. *Anal. Chem.* **1957**, *29*, 916−918.
(33) Zhang, X. S.; Jiang, C.; Cheng, M. J.; Zhou, Y.; Zhu, X. Q.; Nie, J.; Zhang, Y. J.; An, Q.; Shi, F. Facile Method for the Fabrication of Robust Polyelectrolyte Multilayers by Post-Photo-Cross-Linking of Azido Groups. *Langmuir* **2012**, *28*, 7096−7100.
(34) An, Q.; Zhou, Y.; Zhang, Y. J.; Zhang, Y. H.; Shi, F. A Facile Method for the Fabrication of Covalently Linked PAH/PSS Layer-by-Layer Films. *RSC Adv.* **2014**, *4*, 5683−5688.
(35) Zhou, Y.; Cheng, M. J.; Zhu, X. Q.; Zhang, Y. J.; An, Q.; Shi, F. A Facile Method for the Construction of Stable Polymer−Inorganic Nanoparticle Composite Multilayers. *J. Mater. Chem. A* **2013**, *1*, 11329−11334.

DOI: 10.1021/acsami.5b04569
ACS Appl. Mater. Interfaces 2015, 7, 19104−19111

(36) Aisawa, S.; Kudo, H.; Hoshi, T.; Takahashi, S.; Hirahara, H.; Umetsu, Y.; Narita, E. Intercalation Behavior of Amino Acids into Zn−Al-Layered Double Hydroxide by Calcination−Rehydration Reaction. *J. Solid State Chem.* **2004**, *177*, 3987−3994.
(37) Huang, Y. H.; Lu, J.; Xiao, C. B. Thermal and Mechanical Properties of Cationic Guargum/Poly(acrylic acid) Hydrogel Membranes. *Polym. Degrad. Stab.* **2007**, *92*, 1072−1081.
(38) Shi, F.; Liu, S. H.; Gao, H. T.; Ding, N.; Dong, L. J.; Tremel, W.; Knoll, W. Magnetic-Field-Induced Locomotion of Glass Fibers on Water Surfaces: Towards the Understanding of How Much Force One Magnetic Nanoparticle Can Deliver. *Adv. Mater.* **2009**, *21*, 1927−1930.
(39) Rojas, R.; Jimenez-Kairuz, A. F.; Manzo, R. H.; Giacomelli, C. E. Release Kinetics from LDH-Drug Hybrids: Effect of Layers Stacking and Drug Solubility and Polarity. *Colloids Surf., A* **2014**, *463*, 37−43.
(40) Wang, L. J.; Xing, H. Y.; Zhang, S. J.; Ren, Q. G.; Pan, L. M.; Zhang, K.; Bu, W. B.; Zheng, X. P.; Zhou, L. P.; et al. A Gd-doped Mg-Al-LDH/Au Nanocomposite for CT/MR Bimodal Imagings and Simultaneous Drug Delivery. *Biomaterials* **2013**, *34*, 3390−3401.
(41) Gu, Z.; Thomas, A. C.; Xu, Z. P.; Campbell, J. H.; Lu, G. Q. In Vitro Sustained Release of LMWH from MgAl-layered Double Hydroxide Nanohybrids. *Chem. Mater.* **2008**, *20*, 3715−3722.

DOI: 10.1021/acsami.5b04569
ACS Appl. Mater. Interfaces 2015, 7, 19104−19111